Korean J. Chem. Eng., **20**(6), 1123-1130 (2003)

Effects of High Temperature and Combustion on Fluidized Material Attrition in a Fluidized Bed

Chiou-Liang Lin and Ming-Yen Wey†

Department of Environmental Engineering, National Chung-Hsing University, Taichung, 402, Taiwan, R.O.C.
(*Received 3 March 2003 • accepted 12 May 2003*)

Abstract–This study investigated the effects of high temperature and combustion conditions on the attrition of fluidized material in a fluidized bed. Silica sand was fluidized in air at an atmospheric pressure between 873 K and 1,073 K. The operating parameters evaluated in investigating the attrition rate of fluidized material included particle size, temperature and both combustion and non-combustion conditions. Experimental results indicated that the total weight of attrition increased with increasing temperature and decreased with increasing particle size. The attrition was higher during the initial fluidization period than the later period, due to the loss of sharp corners and edges of the attrition particles. The initial and final attrition rates during combustion were higher than those in the non-combustion condition, because the heat and thermal shock were produced to increase attrition rate during incineration. Comparing the experimental data with previous correlations, that reveals a significant level of error in the prediction results from existing correlations. This error may occur because the experimental equations neglected the operating temperature and particle size.

Key words: Gas-solid Fluidized Bed, Attrition, Powder, Combustion, Incineration

INTRODUCTION

The fluidized bed incinerator is the most widespread owing to advantages including good solid mixing, high heat transfer, large contact surface area [Jang et al., 2002] and so on. Accordingly, fluidized beds have been used in several industrial processes, such as combustion [Han et al., 1999; Gu et al., 2002], gasification [Ko et al., 2001; Lee et al., 2002], drying [Choi et al., 2002], coating [Kage et al., 1999] and others. But the attrition/elutriation of bed material is associated with various problems in industrial processing or waste incineration. Attrition increases the number of particles and reduces particle size, which may affect reactor performance, fluidizing properties, fly ash generation, operating stability and operating costs. Fine particles, produced by attrition, are carried out of the combustion chamber with the flue gas, which increases the load of air pollution control devices.

Many previous researches studied the attrition rate of fluidized materials. Particle properties such as porosity, size, hardness, density, surface, and shape influence the attrition rate [Lee et al., 1993], while the operating environment is also an important influence. Ulerich et al. [1980], Vaux and Fellers [1981] and Shamlou et al. [1990] indicated that several mechanisms were responsible for attrition of the fluidized bed, including chemical stress (chemical reactions on the particle surface), thermal stress (unequal temperature and heating/cooling caused by uneven expansion), kinetic stress (the collision of slow-moving or fast-moving particles) and static stress (particle gravity). Arena et al. [1983] and Chirone et al. [1985] indicated that particle sizes were reduced not only by the fluid-dynamic but also by thermal shock and combustion. Wey and Chang [1995] demonstrated that plastic was gasified first, and ignition and burning followed. Meanwhile, the ignition and burning of plastic produced a thermal shock that caused particle attrition. Chirone et al. [1985] and Halder and Basu [1992] pointed out the attrition rate increased when the combustion and attrition exist simultaneously for carbon combustion. However, the effect of gas expansion of ignition and thermal shock on attrition rate had rarely been investigated.

Previous investigations of solid attrition have focused on various operating parameters. Vaux and Schruben [1978], Lin et al. [1980], Shamlou et al. [1990] and Park et al. [2000] found the attrition rate to be a function of excess gas velocity and increase with gas velocity. Finally, Wu et al. [1999] used silica sand as a fluidized material, and showed that particle attrition increased with bed weight. This phenomenon may occur because of the increased pressure fluctuations in deeper beds during slugging. Additionally, particle attrition increased with reducing average particle size due to smaller particles representing a larger number of particles for the same weight basis and having a larger surface area, which increased the probability of collision [Ray and Jiang, 1987; Wu et al., 1999]. To predict the particle attrition rate, previous studies collected their experimental data to develop empirical correlations in different operating conditions, as listed in Table 1 [Gwyn, 1969; Merrick and Highley, 1974; Lin et al., 1980; Wu et al., 1999; Kono, 1981; Halder and Basu, 1992; Cook et al., 1996; Park et al., 2000]. However, most correlations were performed at room temperature, despite the fact that most fluidized applications are conducted at high temperature (for example: solid waste incineration, coal gasification and so on). However, the effect of high temperature and combustion condition on attrition rate had rarely been investigated.

This investigation focused on further assessing the effects of high temperature incineration on the attrition rate of fluidized materials. Fluidization studies were conducted over a temperature range of 873-1,073 K, and particle attrition was measured during combustion or non-combustion conditions. The experimental results will

†To whom correspondence should be addressed.
E-mail: mywey@dragon.nchu.edu.tw

Table 1. Predicted equations of previous researches

Author	Operating conditions	Attrition rate equation		Patricle
Gwyn [1969]	*Particle size (51-260 μm) *Room temperature	$R_t = K_p \times m \times t^{m-1} \times W$	m=0.46 $K_P = 4.47\times10^{-6}$-1.35×10^{-5}	Silica sand
Merrick and Highely [1974]	*Gas velocity (0.6-2.4 m/s) *Bed height (0.6-1.2 m) *Particle size (1,587-3,175 μm)	$R_t = K_a \times (U_0 - U_{mf}) \times W$	$K_a = 4.54\times10^{-3}$-0.015	Limestone
Lin et al. [1980]	*Particle size (37-125 μm) *Gas velocity (0.1-0.3 m/s)	$R_t = 4.683\times10^{-5} \times \exp[0.00162\times(U_0 - U_{mf})] \times W$		Carbon
Kono [1981]	*Particle size (970-4,000 μm) *U/U_{mf} (1.5-5) *Temperature (298-777 K) *Bed diameter (0.1-1.79 m)	$R_t = 2.43\times10^{-9} \times \rho_f \times \overline{U}^3 \times D_t^{0.55} \times W$ $R_t = 8.85\times10^{-9} \times \rho_f \times \overline{U}^2 \times D_t^{0.55} \times W$	For $\overline{U} \le 3.6$ m/s For $\overline{U} > 3.6$ m/s	Silica sand
Halder and Basu [1992]	* Gas velocity (1.7-3.77 m/s) *Temperature (300, 1,073 K) *Sand size (212-355 μm)	$R_t = K_a U_0 W / d_p$	$K_a = 2.57$-4.8×10^{-7} combustion $K_a = 0.03$-0.05×10^{-7} absence combustion condition	Carbon
Cook et al. [1996]	*Gas velocity (1.54-5.0 m/s) *Particle size (903, 1,764 μm)	$R_t = K_a \times \exp[-E_a/(U_0 - U_{mf})^2] \times W$	$E_a = 3.969\times10^{-2}$ kg-m/kg, $K_a = 2.89\times10^{-6}$ s^{-1}	Lime
Wu et al. [1999]	*Particle size (195-421 μm) *Nozzle size (0.003-0.005 m) *Superficial velocity (0.4-1.1 m/s)	$R_t = K_{a0} \times U_0 (U_0 - U_{mf}) \times W/(g \times d_{sv})$ $R_t = K^*_{a0} \times U_0 \times (Q_B/A) \times W$	$K_{a0} = 7.4\times10^{-3}$ s^{-1} $K^*_{a0} = 2.5\times10^{-7}$ s/m^2	Silica sand
Park et al. [2000]	*Particle size (1,400-1,700 μm) *$U\text{-}U_{mf}$ (0.05-0.5 m/s) *Bed height (0.11-0.25 m) *Bed weight (0.6-1.4 kg)	$R_t = 0.01443(U_0 - U_{mf})W - 142.91$		Alumina

be integrated to provide valuable information for selection fluidized materials and operating fluidized bed at high temperature and combustion condition. The adequate design and operating will not only reduce the fly ash but also decrease the investment of air pollution control drives.

EXPERIMENTAL

Fig. 1 illustrates the experimental apparatus. The reactor was a bubbling fluidized bed, comprised of a preheated chamber (length 0.5 m), a main chamber (height 1.1 m) with an inner diameter of 0.09 m, and an expansion section (height 1.0 m) with an inner diameter of 0.25 m. The reactor was constructed of 0.003 m thick stainless steel (AISI 310), and was equipped with a stainless steel porous plate that had a 15% open area to provide gas distribution. The facility was surrounded by electric resistance and packed with ceramic fibers to insulate heat loss. Three thermocouples were used to measure the temperature profile in the preheated chamber, sand bed, and freeboard chamber. The temperature was controlled by a PID controller. Two cyclones were connected to a bag filter to collect the elutriation particles. Silica sand was used as the bed material, and had an almost constant density for all sizes (ρ_p=2,600 kg/m^3). Three particle sizes (545, 770 and 1,095 μm) were prepared by sieve analysis. The height of the static bed was 0.2 m (H/D=2). The experiment was conducted at atmospheric pressure.

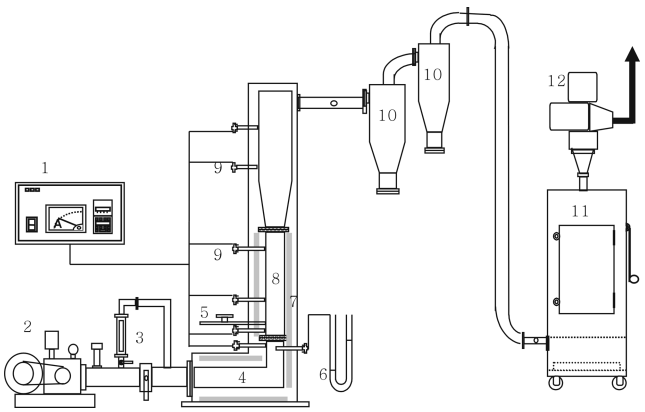

Fig. 1. The bubble fluidized bed incinerator.

1. PID controller
2. Blower
3. Flow meter
4. Preheater chamber
5. Feeder
6. U manometer
7. Electric resistance
8. Solid bed
9. Thermocouple
10. Cyclone
11. Bag filter
12. Induced fan

The temperature was controlled at 873, 973 and 1,073 K, and three types of particle size were studied (545, 770 and 1,095 μm). The operating time was controlled from 0 sec to 14,400 sec. Polypropylene (PP) was selected to simulate waste combustion to understand the effect of thermal shock on the attrition of bed materials. The particle size and density of PP was 0.003 m and 0.96 kg/m^3 individually. Table 2 listed the operating parameters of this experiment.

Before experiments, the operating conditions were checked. When the temperature was controlled at 873 K, the combustion phenomenon of polypropylene (PP) was observed from the top of apparatus. The ignition and combustion flame were observed during combustion. After checking these conditions, we began the formal experiments. The experimental procedure started with preheating the

Table 2. The operating conditions for each experiment

Run	Temperature (K)	Particle size (μm)	Gas velocity (m/s)	Static bed height (m)	Waste	Operating time (sec)
1	873	770	0.176	0.2	No	0-14,400
2	973	770	0.176	0.2	No	0-14,400
3	1,073	770	0.176	0.2	No	0-14,400
4	1,073	545	0.176	0.2	No	0-14,400
5	1,073	770	0.176	0.2	No	0-14,400
6	1,073	1,095	0.176	0.2	No	0-14,400
7	873	770	0.176	0.2	PP	0-14,400
8	973	770	0.176	0.2	PP	0-14,400
9	1,073	770	0.176	0.2	PP	0-14,400
10	1,073	545	0.176	0.2	PP	0-14,400
11	1,073	770	0.176	0.2	PP	0-14,400
12	1,073	1,095	0.176	0.2	PP	0-14,400

solid bed to the operating temperature, after which air was passed through preheated chamber to increase the temperature. The minimum fluidization velocity was determined by the Δp-versus-U_0 diagram. The PP was fed into the incinerator by a feeder at a rate of 1.4×10^{-3} kg per 20 s. The thermocouples send a feedback signal of temperature in the chamber to the PID controller. The PID controller maintains the experimental temperature by controlling the electric resistance. Additionally, during combustion, the combustion plastic releases enough combustion heat to maintain the experimental temperature, and the PID controller is used only to raise the temperature before experimentation. Fig. 2 shows the temperature profile of combustion and non-combustion conditions. After the predetermined operating time (initially the incinerator was stopped every 600 sec, then after 1,800 sec it was stopped every 1,800 sec), the incinerator was stopped and cooled for 25,200 sec. When the incinerator cooled to room temperature, the residual bed materials were collected and elutriation particles were also collected by the cyclones and bag filter. The residual bed materials were weighed, put into the bed, and the above steps repeated. The total operating time was 14,400 sec. The attrition rate was assumed to be the same as the elutriation rate because the terminal velocity of the particles always exceeded the superficial gas velocity in this experiment. This assumption was used in previous studies by Ray and Jiang [1987], Kono [1981] and Chu et al. [2000]. After 14,400 sec, the residual bed materials were sieved to analyze the particle size distribution.

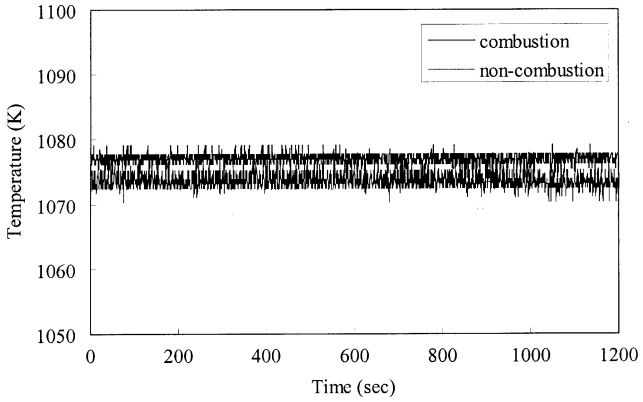

Fig. 2. The temperature profile of combustion and non-combustion conditions.

1. Estimation of the Attrition Rate of Solids

According to a previous study [Wu and Chu, 1998], the material balance for fine particles was as follows:

(Initial input, actual generation)=Output+Accumulation

$$F_{0(fine)} = F_{2(fine)} + \frac{dW_{(fine)}}{dt} \tag{1}$$

Solving the above equation gives the weight of fines in the bed as a function of time

$$W_{(fine)} = \frac{F_{0(fine)}}{K_{(fine)}}[1-e^{-K_{(fine)}t}] + W_{0(fine)}e^{-K_{(fine)}t} \tag{2}$$

The total carryover balance of fines

total carryover=(initially in bed)+(flow in from t=0)−(in bed at time t)

Rearranging the above equation gives the fines in the carryover stream

$$W_{(fine\ in\ carryover)} = \left[W_{0(fine)} - \frac{F_{0(fine)}}{K_{(fine)}}\right]\cdot[1-e^{-K_{(fine)}t}] + F_{0(fine)}t \tag{3}$$

$K_{(fine)}$, $W_{0(fine)}$ and $F_{0(fine)}$ are unknowns, and can be found by using

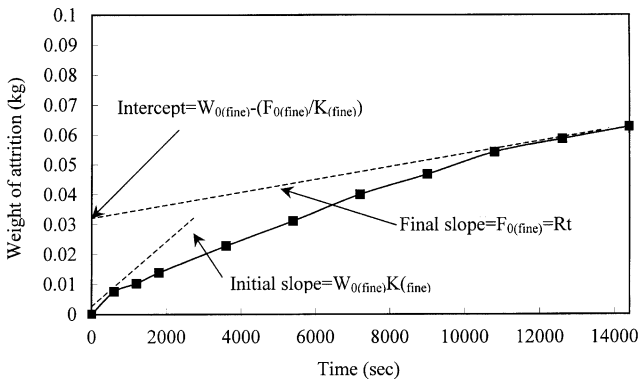

Fig. 3. Removal of fines from a bed, during batch operations (The operating conditions at 973 K, 770 μm and non-combustion).

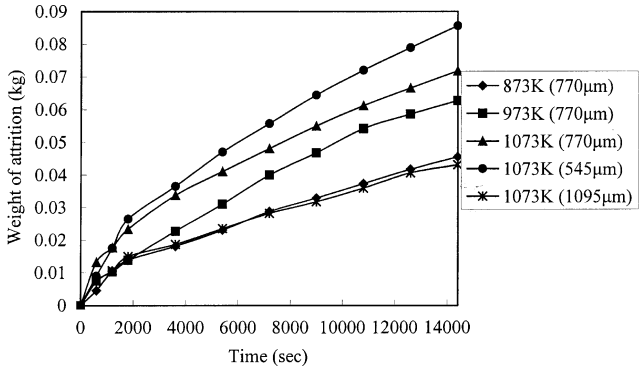

Fig. 4. The effect of operating temperature and particle size on particle attrition at non-combustion condition.

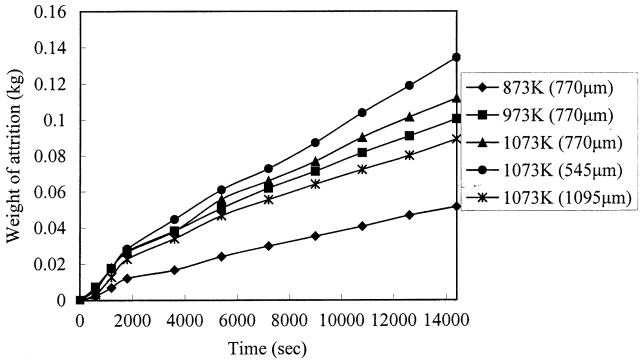

Fig. 5. The effect of operating temperature and particle size on particle attrition at combustion condition.

Eq. (3). The slope and intercept of Fig. 3, which is a typical experiment, can be used to calculate these unknowns.

RESULTS AND DISCUSSION

1. Particle Attrition of Different Operating Parameters in the Non-combustion Condition

Fig. 4 shows the effect of operating temperature and particle size on particle attrition in the non-combustion condition. After 7,200 sec, the weight loss of the bed material tends to become constant. The results indicate the total weight of attrition increases with increasing temperature and decreases with increasing particle size. Particle attrition increases with decreasing average particle size, due to smaller particles representing a larger number of particles for the same weight basis, and also having more surface area, increasing the probability of collision [Ray and Jiang, 1987; Wu et al., 1999]. Ray and Jiang [1987] developed a "surface-reaction" model, which states that attrition is proportional to particle surface area. The attrition fraction of smaller particles increases with decreasing particle size for the same materials. Additionally, the motion of fine particles is faster than that of coarse particles at the same gas velocity. Meanwhile, kinetic stress increases as the motion of particles, thereby increasing the rate of particle collision and attrition.

Particle attrition increases with the operating temperature owing to thermal stress. The unequal temperature heats particles to cause uneven expansion and the possibility of decrepitation. At high temperatures, the minimum fluidization velocity decreases [Wu and Baeyens, 1991]. At the same air flow rate, particles move faster at high temperature than that at low temperature, increasing both the thermal and kinetic stress at high operating temperature and also increasing particle attrition.

2. Comparison of Particle Attrition Rate in Both Combustion and Non-combustion Situations

Fig. 5 displays the results of attrition during combustion. Attrition increases with temperature and decreases with increasing particle size. Comparing Fig. 4 and Fig. 5 reveals that the total attrition during combustion is significantly higher than that in the non-combustion condition. High combustion temperature and thermal shock enhance attrition. Wey and Chang [1995] showed the plastic was gasified first, and ignition and burning then followed. The organic gas ignites as its ignition point is reached, and the expansion of volatiles in the porous structure of particles causes particle disintegration.

Halder and Basu [1992] investigated carbon attrition during combustion, and found that attrition is enhanced by combustion. The thermal stress of combustion and thermal shock may increase the breaking force and induce the disintegration mechanism. When a particle disintegrates into two parts, the particle surfaces are splitting. The splitting corners and edges tend toward attrition to make the particle surface smooth and spherical. Therefore, most fine particles were produced by attrition under circumstances of combustion and thermal shock.

Figs. 6 and 7 show the particle attrition rate during combustion

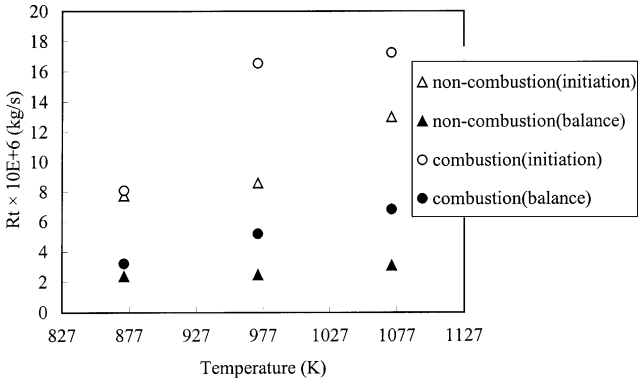

Fig. 6. The attrition rate of combustion and non-combustion at different temperature and particle size is 770 μm.

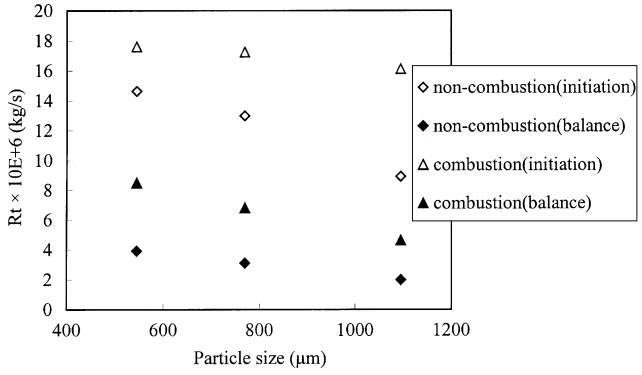

Fig. 7. The attrition rate of combustion and non-combustion at different particle size and temperature is 1,073 K.

and non-combustion. According to the calculation results, the rate of weight loss by elutriation is smaller than that by attrition during the later period. Because the fluidized materials were screened before experiment, we assumed these bed materials did not contain any fines. So the particle weight by elutriation was similar to the weight of particle by attrition during initial fluidization. Vaux and Kearins [1980] and Patel et al. [1986] investigated the attrition of non-spherical particles, and found a high rate of fine formation during initial fluidization, due to the loss of sharp corners and edges of the attrition particles. When particles gradually become rounded, the rate of attrition tends toward a constant. Additionally, Lee et al. [1993] indicated that the sharp edges gradually disappear and the particle form gradually tends to sphericity. According to our results, the attrition rate during initial fluidization is higher than that during later period. This result agrees with previous results. According to pictures of sand particles of SEM, which are shown in Fig. 8, the pictures (Fig. 8a) and (Fig. 8c) showed the fresh sand particle before experiment. From (Fig. 8a) and (Fig. 8c), the sharp corners and edges were observed significantly. After experiment, the pictures were shown in (Fig. 8b) and (Fig. 8d), the surface and shape of particle became smooth and sphericity. The sharp corners and edges of sand particle were lost after attrition. Therefore, we speculate the loss of sharp corners and edges of the particle increase attrition rate. Then, particles gradually tend to sphericity and cause attrition to become constant gradually. So, the ash produced by attrition is higher during initial fluidization period than during the later period.

In the non-combustion condition, high temperatures (973 K and 1,073 K) affect attrition rate mainly during initial fluidization. Thermal stress is important at high temperatures, but its influence gradually decreases with increasing temperature. The attrition rate of the combustion condition is higher than that of the non-combustion condition. The combustion heat and thermal shock affect the attrition rate of bed materials. However, at 873 K the attrition rate of combustion approaches that of non-combustion. This phenomenon occurs because of the combustion process of PP, which cracks organic components slowly at low temperature (873 K), and the organic gas is carried with fluidized gas from the PP surface. The combustion is thus appeased and the thermal shock is insignificant. At high temperatures (973 K and 1,073 K), gasification occurs quickly, the ignition point is immediately reached, and the organic gas explodes. The ignition and burning of plastic caused thermal shock and particle attrition.

Comparison of the above results reveals that regardless of the parameters used, the attrition rate is higher during initial fluidization than at other times. Consequently, ash is produced largely when the incinerator starts and renews fluidized bed material. The size of the fluidized bed material is important, and influences the creation of ash from attrition. Using coarse particles can decrease attrition.

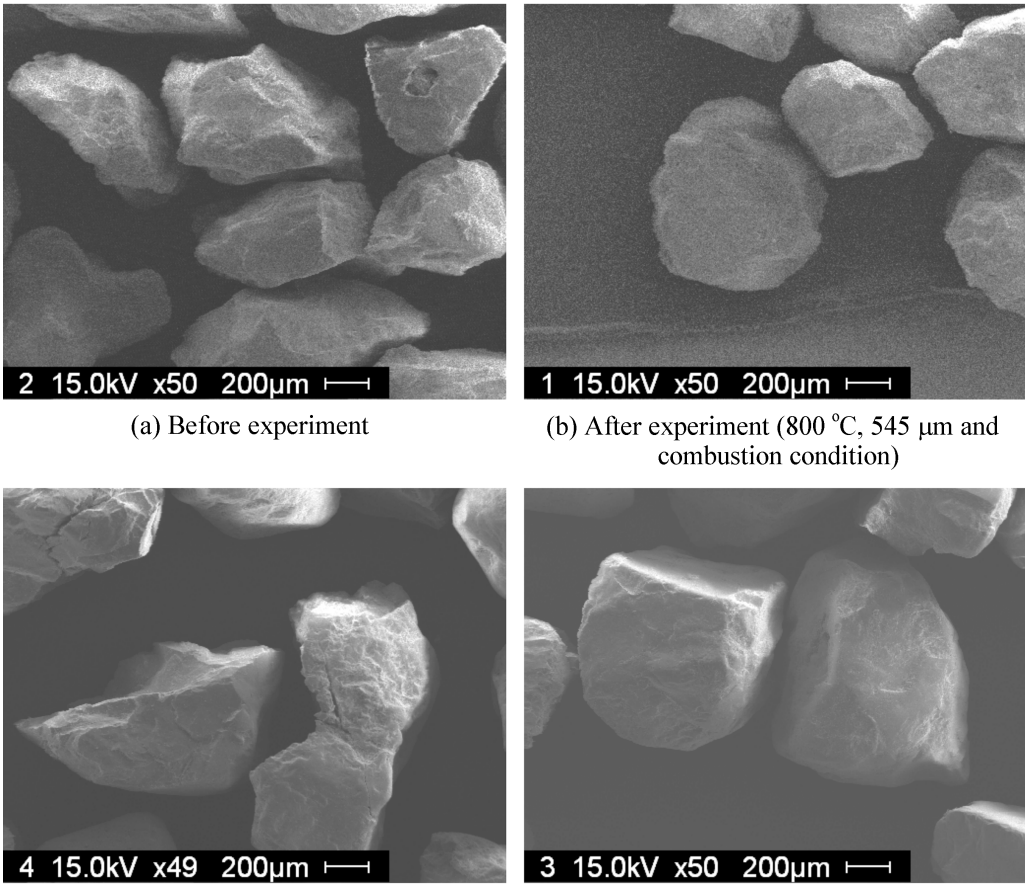

(a) Before experiment

(b) After experiment (800 °C, 545 μm and combustion condition)

(c) Before experiment

(d) After experiment (800 °C, 770 μm and combustion condition)

Fig. 8. The pictures of sand particle of SEM before and after experiment.

Geldart [1973] classified four types of powder (A, B, C and D) according to size and density. The coarsest particles (1,095 μm), classified as type D, have poor solid mixing and fluidized quality and spout easily. The use of D powder as a fluidized material reduces combustion efficiency.

3. Comparison of Experimental Data and Predictions by Empirical Equations

Table 1 lists previous empirical correlations used to predict the attrition rate for different particles. Notably, most correlations were developed with experimental data, which were sampled at room temperature. To compare prediction values with the attrition rate measured by this investigation at high temperature, empirical correlations, such as those presented by Gwyn [1969], Kono [1981] and Wu et al. [1999] are used for the calculations, because these equations were developed based on silica sand.

Figs. 9 and 10 display the calculation results and compare them with the experimental data at high temperature and different particle size obtained in this investigation. The comparison reveals that the prediction results based on existing correlations differ significantly from the experimental data. This discrepancy occurs because almost all investigators developed their empirical correlations based on the gas velocity, and neglected the effect of temperature and particle size. However, the variation of attrition rates with particle size and temperature confirms other observations that gas velocity is not only an important parameter in predicting attrition rate.

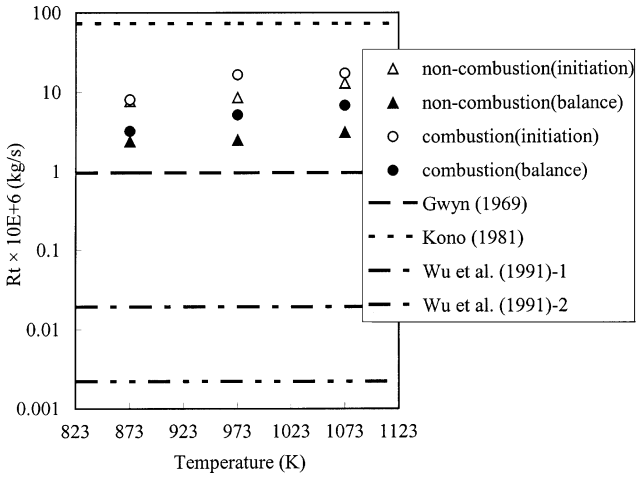

Fig. 9. The results of predicted compared with experimental attrition rate of different temperature (particle size 770 μm).

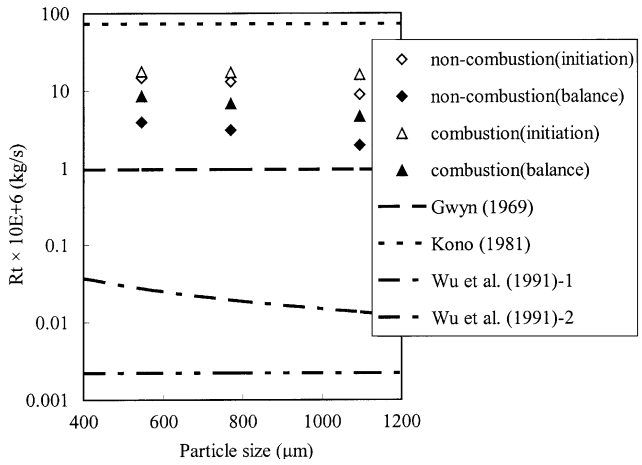

Fig. 10. The results of predicted compared with experimental attrition rate of different particle size (temperature 1,073 K).

4. Size Distribution of Different Operating After the Experiments

In order to observe the change of particle size, the all bottom bed materials after experiment were segregated by sieve analysis. Though, the sieve analysis is unlike the accuracy of electronic or laser analysis methods, but it adapts to analyze a large amount of sand materials. If electronic or laser analysis methods are used, the sampling error may influence significantly because a little sample may not represent all bed materials. In order to compare the results of before and after experiment and prevent sampling error, the sieve analysis was used to analyze the particle size distribution after experiment.

Therefore, Fig. 11 illustrates the results of sieve analysis and compares them with temperature and combustion. The figure contains two peaks besides 770 μm, namely 545 μm and 350 μm. Meanwhile, the thermal stress and thermal shock may increase breaking force and cause the breaking mechanism to disintegrate into two parts. The fine and a single son particle are produced, and the new particle is only slightly smaller than original particle [Ray and Jiang, 1987]. Consequently, we hypothesize that the two peaks in the figure represent the division of son and fine particles.

The above discussion indicates that the production of thermal shock and combustion heat enhances attrition in the combustion condition. According to Fig. 11, the 770 μm reduces significantly and largely produces numerous son and fine particles. Furthermore, the breaking mechanism frequently emerges in the combustion condition. However, at 873 K, the effect of thermal shock on the breaking mechanism is insignificant during combustion, owing to particle size distribution being similar in both conditions. The reason is because of the process of PP combustion, which cracks organic components slowly at low temperature (873 K), while the organic gas is carried with fluidized gas from the PP surface. The combustion is thus appeased and the thermal shock is insignificant.

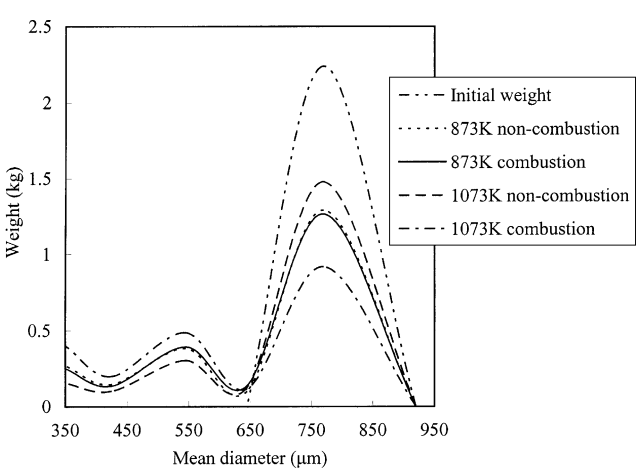

Fig. 11. The result of sieve analysis compared with initial weight at different condition.

CONCLUSION

This study investigates the effect of high temperature and combustion condition on fluidized material attrition in fluidized bed, and uses different parameters, such as particle size, combustion temperature and non-combustion, to study the attrition rate of fluidized materials. The analytical results demonstrate that particle attrition increases as average particle size decreases and operating temperature increases.

Comparing the results for combustion with those for non-combustion reveals that total weight of attrition during combustion is significantly higher than under the non-combustion condition, because the combustion heat and thermal shock increase attrition. The attrition rate of particles is higher during initial fluidization than during the later period, and the loss of sharp corners and edges of the attrition particles gradually causes attrition to become constant gradually. Comparing experimental data with previous correlations reveals a significant level of error in the predicted results from existing correlations. This error may occur because the experimental equations neglected the operating temperature and particle size, which concerned gas velocity importantly.

NOMENCLATURE

A : cross-sectional area of the bed [m^2]
d_p : average particle diameter [m]
d_{sv} : average sieve cut size [m]
D_t : diameter of fluidized bed [m]
E_a : attrition activation energy [kg-m/kg]
$F_{0(fine)}$: fictitious feed stream of fines [kg/s]
$F_{2(fine)}$: total fines carried out of the bed since t=0 [kg/s]
g : acceleration due to gravity [m/s^2]
$K_{(fine)}$: elutriation rate constant of fines [1/s]
K_a : attrition rate constant [1/s]
K_{a0} : intrinsic attrition constant [1/s]
K^*_{a0} : intrinsic attrition constant [s/m^2]
K_p : dimensional constant, unit t^{-m}, in mass rate equation
L_e : height of expanded fluidized bed [m]
m : exponent for time dependence of attrition [-]
Q_B : visible bubble volume [m^3/s]
Rt : attrition rate [kg/s]
t : attrition time [s]
$\overline{U}$: effective gas velocity [m/s]
U_0 : superficial gas velocity [m/s]
U_{mf} : minimum fluidization velocity [m/s]
W : weight of solids [kg]
$W_{0(fine)}$: initial weight of fines in the bed [kg]
$W_{(fine\ in\ carryover)}$: total mass of particles carried [kg]
ρ_p : solids density [kg/m^3]
ρ_f : density of fluidizing gas [kg/m^3]

REFERENCES

Arena, V., D'Amore, M. and Massimilla, L., "Carbon Attrition during the Fluidized Combustion of a Coal," *AIChE J.*, **29**, 40 (1983).

Chirone, R., D'Amore, M., Massimilla, L. and Mazza, A., "Char Attrition during the Batch Fluidized Bed Combustion of Coal," *AIChE J.*, **31**, 812 (1985).

Choi, K. B., Park, S. I., Park, Y. S., Sung, S. W. and Lee, D. H., "Drying Characteristics of Millet in a Continuous Multistage Fluidized Bed," *Korean J. Chem. Eng.*, **19**, 1106 (2002).

Chu, C. Y., Hsueh, K. W. and Hwang, S. J., "Sulfation and Attrition of Calcium Sorbent in a Bubbling Fluidized Bed," *J. of Hazardous Materials*, **B80**, 119 (2000).

Cook, L. J., Khang, S. J., Lee, S. K. and Tim, C. K., "Attrition and Changes in Particles Distribution of Lime Sorbents in a Circulation Fluidized Bed Absorber," *Powder Technol.*, **89**, 1 (1996).

Geldart, D., "Types of Gas Fluidization," *Powder Technol.*, **7**, 285 (1973).

Gu, J. H., Yeo, W. H., Seo, Y. C., Lee, S. H. and Lee, J. K., "The Characteristics of Co-incineration of Dewatered Sludge, Waste Oil and Waste Solvent in Commercial-scale Fluidized Bed Incinerator," *Korean J. Chem. Eng.*, **19**, 324 (2002).

Gwyn, J. E., "On the Particle Distribution Function and the Attrition of Cracking Catalysts," *AIChE J.*, **15**, 35 (1969).

Halder, P. K. and Basu, P., "Attrition of Spherical Electrode Carbon Particles during Combustion in a Turbulent Fluidized Bed," *Chem. Eng. Sci.*, **47**, 527 (1992).

Han, K. H., Park, J., Ryu, J. I. and Jin, G. T., "Coal Combustion Characteristics in a Pressurized Fluidized Bed," *Korean J. Chem. Eng.*, **16**, 804 (2001).

Jang, J. G., Kim, M. R., Lee, K. H. and Lee, J. K., "Enhancement of Combustion Efficiency with Mixing Ratio during Fluidized Bed Combustion of Anthracite and Bituminous Blended Coal," *Korean J. Chem. Eng.*, **19**, 1059 (2002).

Kage, H., Dohzaki, M., Ogura, H. and Matsuno, Y., "Powder Coating Efficiency of Small Particles and Their Agglomeration in Circulating Fluidized Bed," *Korean J. Chem. Eng.*, **16**, 630 (1999).

Ko, M. K., Lee, W. Y., Kim, S. B., Lee, K. W. and Chun, H. S., "Gasification of Food Waste with Steam in Fluidized Bed," *Korean J. Chem. Eng.*, **18**, 961 (2001).

Kono, H., "Attrition Rate of Relatively Coarse Solid Particles in Various Types of Fluidized Beds," *AIChE Symp. Ser.*, **77**, 96 (1981).

Lee, S. K., Jiang, X., Keener, T. C. and Khang, S. J., "Attrition of Lime Sorbents during Fluidization in a Circulating Fluidized Bed Absorber," *Ind. Eng. Chem. Res.*, **32**, 2758 (1993).

Lee, W. J., Kim, S. D. and Song, B. H., "Steam Gasification of an Australian Bituminous Coal in a Fluidized Bed," *Korean J. Chem. Eng.*, **19**, 1091 (2002).

Lin, L., Sesrs, J. T. and Wen, C. Y., "Elutriation and Attrition of Char a Large Fluidized Bed," *Powder Technol.*, **27**, 105 (1980).

Merrick, D. and Highley, J., "Particle Size Reduction and Elutriation in a Fluidized Bed Process," *AIChE Symp. Ser.*, **70**, 366 (1974).

Park, Y. S., Kim, H. S., Shun, D., Song, K. S. and Kang, S. K., "Attrition Characteristics of Alumina Catalyst for Fluidized Bed Incinerator," *Korean J. Chem. Eng.*, **17**, 284 (2000).

Patel, K., Nienow, A. W. and Milne, L. P., "Attrition of Urea in a Gas-Fluidized Bed," *Powder Technol.*, **47**, 257 (1986).

Ray, Y. C. and Jiang, T. S., "Particle Attrition Phenomena in a Fluidized Bed," *Powder Technol.*, **49**, 193 (1987).

Shamlou, P. A., Liu, Z. and Yates, J. G., "Hydrodynamic Influences on Particle Breakage in Fluidized Beds," *Chem. Eng. Sci.*, **45**, 809 (1990).

Ulerich, N. H., Vaux, R. A., Newby, R. A. and Keairns, D. L., Experimental/Engineering Support for EPA's PBC Program, Final Rep., EPA-600/7-80-015A, Westinghouse Research and Development

Center, Pittsburgh, PA, USA, Jan. (1980).
Vaux, W. G. and Fellers, A. W., "Measurement of Attrition Tendency in Fluidization," *AIChE Symp. Ser.*, **77**, 107 (1981).
Vaux, W. G. and Kearins, D. L., in "Fluidization," Grace, J. R. and Matsen, J. M., Eds., Plenum Press, New York, 437 (1980).
Vaux, W. G. and Schruben, J. S., "Kinetics of Attrition in the Bubbling Zone of Fluidized Beds," *AIChE J.*, **79**, 97 (1978).
Wey, M. Y. and Chang, C. L., "Kinetic Study of Polymer Incineration," *Polymer Degradation and Stability*, **48**, 25 (1995).
Wu, S. Y. and Baeyens, J., "Effect of Operating Temperature on Minimum Fluidization Velocity," *Powder Technol.*, **67**, 217 (1991).
Wu, S. Y. and Chu, C. Y., "Attrition in a Gas Fluidized Bed with Single High Velocities Vertical Nozzle," World Congress on Particle Technology 3rd, Brighton, U.K., 152 (1998).
Wu, S. Y., Baeyens, J. and Chu, C. Y., "Effect of the Grid-Velocity on Attrition in Gas Fluidized Beds," *Can. J. of Chem. Eng.*, **77**, 738 (1999).